16th World Conference on Earthquake, 16WCEE 2017

Santiago Chile, January 9th to 13th 2017

Paper N° 3870

Registration Code: S-XXXXXXXX

ECCENTRIC LEVER ARM AMPLIFICATION SYSTEM FOR FRICTIONAL ENERGY DISSIPATION DEVICES

José Luis Almazán(1), Nicolás Tapia(2), Juan Baquero(3).

(1) *Ph.D., School of Engineering, Pontificia Universidad Católica de Chile, jlalmaza@ing.puc.cl*
(2) *M.Sc., School of Engineering, Pontificia Universidad Católica de Chile, nftapia@uc.cl*
(3) *M.Sc., School of Engineering, Pontificia Universidad Católica de Chile, jsbaquero@uc.cl*

Abstract

Recent analytic, experimental, and practical studies are developing energy dissipation devices combined with amplifying mechanisms (AM) to enhance the seismic perfomance of structures with small inter-story deformations. This research presents the theoretical

and experimental development of the Eccentric Lever-Arm System (ELAS), a new system which is a combination of an AM with one or more dampers capable of supporting large deformations. This work is divided in four parts: (1) kinematics of the ELAS and definition of an equivalent system without AM; (2) parametric analysis of a linear single-story structure with ELAS; (3) numerical analysis of a stiff multi-degree of-freedom structure with two types of frictional dampers; and (4) pseudo-dynamic tests of a full

scale asymmetric one story steel structure with and without frictional dampers. Parametric analyses demonstrate that using high amplification ratios and low supplemental damping could be a very good practice . On the other hand, similar to systems without AMs, dissipation efficiency increases conformably with the stiffness of the secondary structure. As expected, it was observed that deformation was highly concentrated in the flexible edge of the asymmetric test model without damper. Conversely, the structure with frictional AAD clearly showed uniform plane deformation (i.e. tosional balance). The implemented AM, which has a large amplifying ratio of 11, performed with close accordance with numerical simulations.

Keywords: eccentric lever-arm system, Added stiffness and damping, Amplifying mechanism, Torsional balance, Pseudo-dynamic test, Seismic protection, structural response.

1. Introduction

The application of the classical concepts of vibration control by mean of passive energy dissipation devices (EDD), has been widely developed in the field of earthquake engineering [1–3]. However, the use of EDDs has not achieved widespread acceptance in professional practice. This situation could be attributed to two causes: (1) the cost of implementation of the EDDs is still relatively high; and (2) reductions in the maximum inter-story deformation (for example) rarely exceeds 30%. In other words, the cost/benefit ratio is not yet attractive enough to designers and owners, especially in developing countries. Clearly, steel framed structures take more advantage of the use of EDDs, especially medium and high rise buildings located in soft soils (i.e. narrow band seismic motion). On the other hand, reinforced concrete walled structures located in firm soil (i.e. broad band seismic motion) show greater difficulties in the successful implementation of EDDs. In earthquake engineering applications, the most commonly used energy dampers are: (1) hysteretic metal dampers [4–12]; (2) frictional dampers [13–18]; and (3) non-linear viscous dampers [19–21]. While few applications in real structures are known, they have also proposed many semi-active devices for control of vibration in structures. Among them we can mention a system controlled by an electromechanical actuator capable of independently varying stiffness (SAIVS) [22], damping (SAIVD) [23], or frictional force (SAIVF) [24]. Moreover, it has recently been proposed a non-linear passive system called adaptive negative stiffness (ANSS) [25,26] designed to introduce an effect of ‘‘apparent weakness” in the structure due to the unloading of a pre-compressed spring.

Despite the variety of EDDs, the economic factor remains very important, being necessary to optimize the quantity, unit cost, and its location within the structure. For this reason, and due to its simplicity and (relative) lower cost, frictional and metal devices are currently the most used ones in professional practice.

To overcome the problem of small inter-story deformations, various amplifying mechanisms have been proposed, among which we can mention the ‘‘toggle brace damper” (TBD) [27–30], ‘‘scissorjack” [31], ‘‘lever-arm” [32], hydraulic amplification device [33], and amplification systems based on pinions of different diameters [34]. Of all the devices mentioned above, the TBC is probably the most studied, both analytically and experimentally. Furthermore, it is the only amplifying mechanism which real applications have been reported [35,36]. In Ref. [27], a shaking table test of a onestory half-scale model is presented. The results of this study show that the TBD is an easy to design mechanism, of relatively simple construction, and capable to reach real amplification values between 2 and 3.

On the other hand, the EDDs has arisen as one of the most advisable solutions to control deformations in asymmetric structures. There is a large number of numerical studies regarding the effectiveness of EDDs to control torsional effects in asymmetric structures subjected to earthquakes [37–39]. In the context of linear single story structures with viscous damper, the so-called ‘‘mirror rule” [37] was the first criterion proposed in the literature related to the optimal plan location of the EDDs. This concept suggests that the center of supplemental damping (CSD) and the center of stiffness (CS) should be placed at equal distance and in opposite side from de center of mass (CM). Later, the ‘‘torsional balance” concept was proposed as a general design criterion for linear and nonlinear asymmetric structures with linear and non-linear EDDs [40–42]. Torsional balance is defined as the property of an asymmetric structure that leads to equal deformation demand in structural members equidistant from the geometric center (GC) of the structure plan. By mean of shaking table tests of small-scale asymmetric models [43,44], the torsional balance concept has been experimentally proved. Nevertheless, full-scale experimental studies of asymmetric structures with EDDs subjected to seismic excitations have not been reported in the literature.

This research presents the theoretical and experimental development of a new system of eccentric lever arm amplification system, which is combined of a traditional frictional damper and a frictional self-centering damper capable to support large deformations. The work is divided in three parts: (1) proposed amplification system; (2) pseudodynamic tests of a full scale asymmetric one story steel structure and details of the two dissipation devices used; (3) Results obtained. The main hypothesis of this work is that the use of frictional dissipation devices, combined with amplification systems, are an efficient alternative for structures based on frames, as well as, and especially in structures based on reinforced concrete walls (typical building in Chile), where the relatively small story-drift makes it difficult to implement EDDs.

2. Proposed amplifying mechanism

The proposed amplifying mechanism (AM), is a variant of the already known lever-arm system (LAS) [45]. **Fig.1a** shows schematically a typical configuration for the proposed AM, which is denominated as Eccentric Lever-Arm System (ELAS). In this configuration only one damper is used (concentrated damping). There are two main differences between these systems: (i) in the LAS mechanism, the lever-arm is symmetrically located in the center of the frame bay, with one of its ends connected to the middle point of the beam while in the ELAS mechanism, the lever-arm is located at one side of the frames bay (here is where the name “eccentric” comes from) and directly connected to the frame beam-column joint; and (ii) while the LAS mechanism is installed coupled to a V-shaped secondary structure (chevron), the ELAS is installed coupled to only one diagonal bar.

Fig.1b shows other possible configuration for the ELAS. This one is made up of two diagonals (bars or cables), two lever-arms and one horizontal bar (coupling bar), which connects the free ends of the two lever-arms. This configuration is especially convenient when a group of energy dissipation devices is meant to be installed (distributed damping system), being these connected to the coupling bar. It is important to notice that for this configuration, the diagonal bar can be replaced by cables (tension-only). This is possible because the coupling bar transmits the displacement in both directions (case shown in Figure 2b), whatever cable is “activated”.

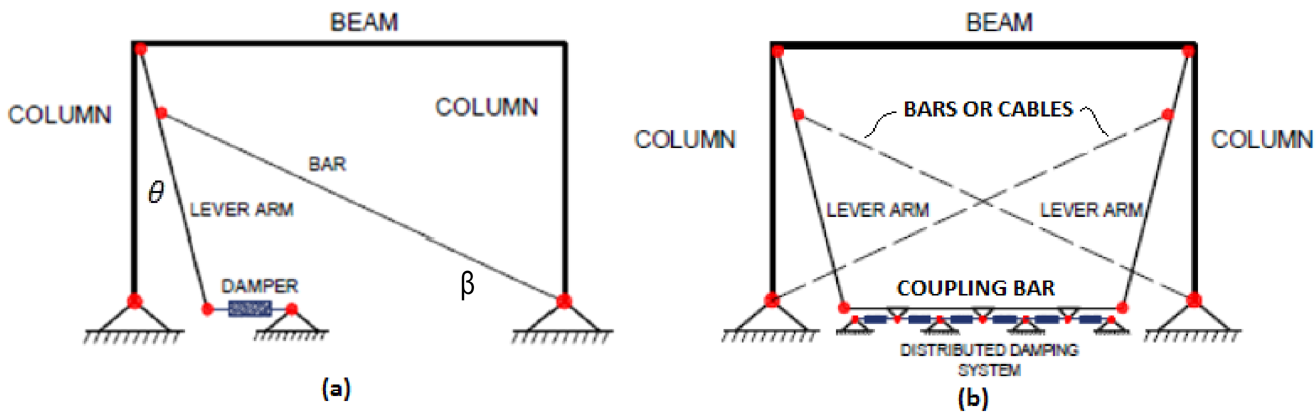

Fig 1. Eccentric Lever-Arm System (ELAS); (a) one damper (concentrated energy dissipation); and (b) various dampers (distributed energy dissipation).

Since the elements of the mechanism are assumed undeformable in this kinematic analysis, we can use the concept of instantaneous center of rotation (ICR) to calculate a_{tg} [45].

$$\alpha_{tg} = \frac{a+b}{a}\frac{cos\theta cos\beta}{cos\beta} - 1 = (\alpha+1)\frac{cos\theta cos\beta}{cos\beta} - 1 \tag{1}$$

3. Pseudo-dynamic tests of a full scale asymmetric one story steel structure

To evaluate the efficiency of proposed amplifying mechanism with added stiffness and damping (AASD) [46], a full-scale onestory steel structure was built. **Fig.2** shows an isometric view, a plan view of the upper diaphragm, and a photograph of the assembled structure in the new Laboratory of Structural Engineering of the Pontificia Universidad Católica de Chile. This laboratory has been recently equipped with a 10 m x 10 m in plan, and 1 m depth concrete reaction slab; a post-tensioned, L-shaped concrete reaction wall of 10 m length, 5 m height, and 0.8 m width; and a multi-axis pseudo-dynamic system (MA-PSDS). The four columns have a section HN30x106, while the peripheral and interior beams have a section IN25x32.6 and IN20x19.8, respectively. In order to generate a reconfigurable and easy to assemble (and to disassemble) structures, all connections are bolted. A490 5/8” bolt connections for flange, and A490 ½” bolt connections to web, were used. The interior beams were connected only in the web. In order to localize (and identify) possible inelastic deformations, the ends of the peripheral beams and column bases have reduced sections. Note that the columns are oriented so that the structure is nominally symmetric, and with the same nominal stiffness in both directions.

The MA-PSDS consists of: (1) 50 kW Hydraulic Power Supply, capable of supplying an oil flow of 100 l/min at 240 bar pressure; (2) Hydraulic Service Manifold, capable of operating at low and high pressure; (3) four hydraulic actuators; and (4) PID control system and data acquisition. In this research we have only used the three actuators. The location and orientation of these actuators can simultaneously control the three degrees of freedom (DOF) of the diaphragm: two horizontal displacements and plan rotation. The actuators #1 and #2, located at Axis 3 and 5, respectively, has a 320/600 kN of load capacity (tension/compression), and ±50 mm of displacement capacity. The actuator #3, located at Axis C, have the same force capacity, and ±200 mm of displacement capacity. **Fig.3** shows a scheme of the amplifying mechanism used in this research, which is named as eccentric lever arm system (ELAS) [45] and a photograph of the AASD installed at the axis-A of the structure. The amplifying mechanism has a theoretical amplification ratio of a = 11.

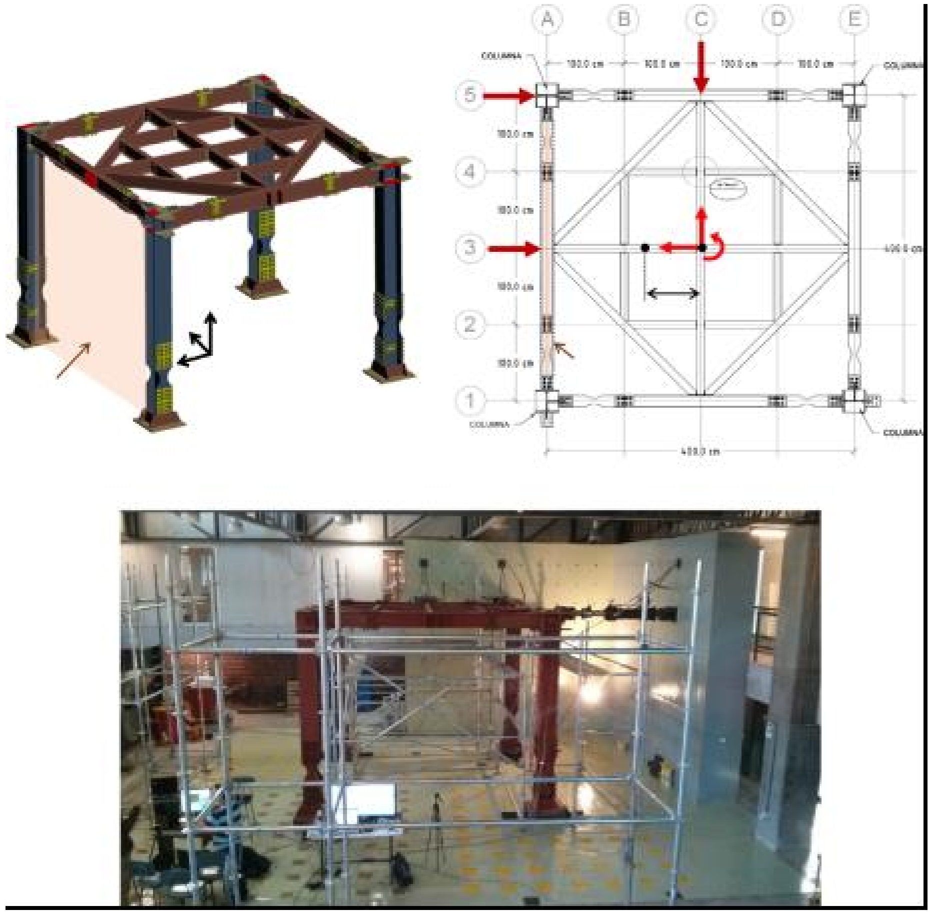

Fig 2. Full scale one-story steel structure: (a) isometric view; (b) plan view of the upper diaphragm; and (c) photograph of the structure and pseudo-dynamic setup at the new Laboratory of Structural Engineering of Pontificia Universidad Católica de Chile.

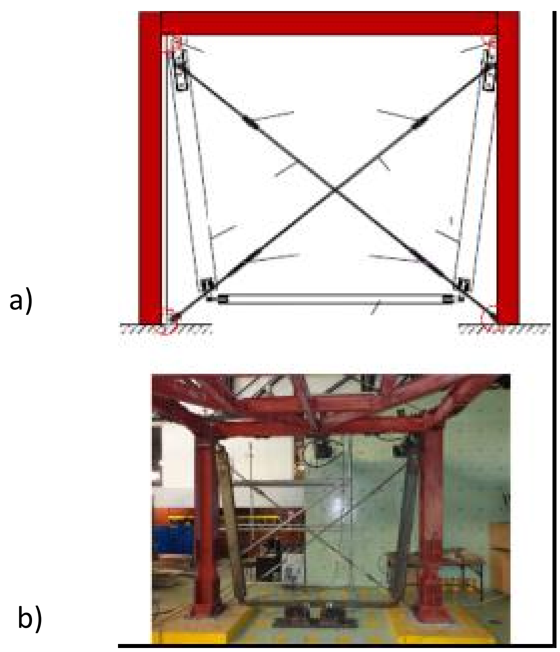

Fig 3. (a) Scheme of the eccentric lever arm system (ELAS) used as amplifying mechanism; and (b) photograph of the AASD installed at axis-A of the structure.

To identify the stiffness matrix of the structure, controlled movements in each DOF of the diaphragm were imposed, maintaining in zero the other two DOFs. **Fig.4** shows the measured force–deformation relationships of the structure without AASD, obtained by quasi-static cyclic tests of increasing amplitude. A hysteretic behavior in the 3 DOFs was observed, associated to sliding of the bolted joints. The figure shows the equivalent stiffness k_{eq} and equivalent damping ratio ξ_{eq}, corresponding to the cycle of maximum deformation of each test. Note that the equivalent damping ratio in X-DOF (ξ_{eq} = 0.19) is 54% higher than in the Y-DOF (ξ_{eq} = 0.123), which is due to the applied load in X-DOF is concentrated in a single actuator, generating more sliding in the bolted connections of the peripheral and interior beams. The reduced sections, both beams and columns, are kept in elastic range.

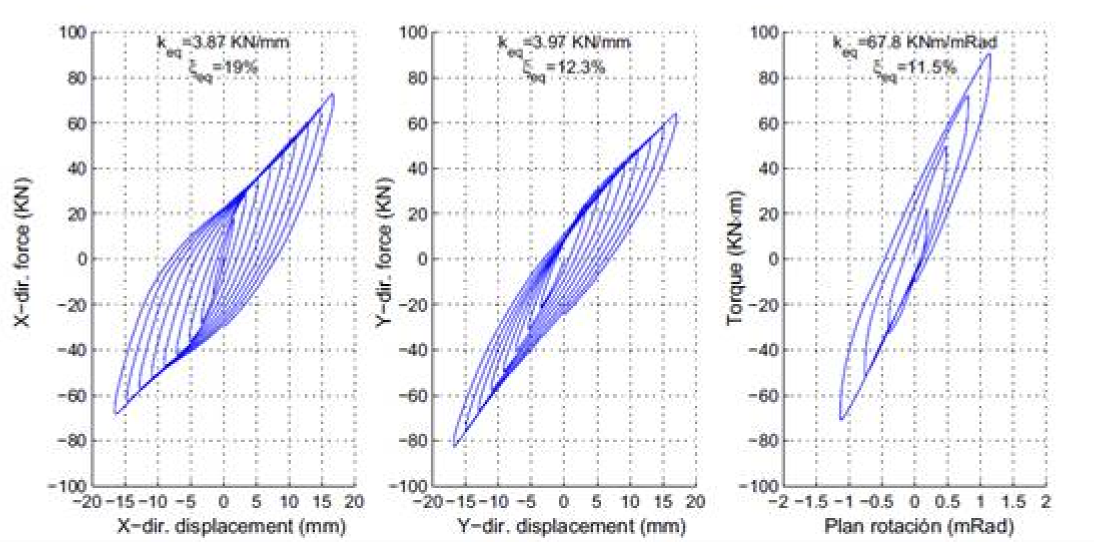

Fig 4. Measured force–deformation relationships of the structure without AASD in X-DOF (left), Y-DOF (center), and torsional-DOF (right).

One of the great advantages of the pseudo-dynamic tests is that the mass matrix of the structure is simulated computationally [49– 55]. This is especially useful when trying to simulate torsional effects, because we can arbitrarily change the amount of mass and its spatial distribution. The mass matrix considered for the structure is equal to:

$$\mathbf{M} = m\begin{bmatrix} 1 & 0 & -e_y \\ 0 & 1 & 0 \\ -e_y & 0 & \rho^2 \end{bmatrix} \tag{2}$$

where m = 30 ton is the translational mass; e_y = 0.8 m is the mass eccentricity; and ρ = 2.35 m mass radius of gyration. Since the structure without AASD has its own internal energy dissipation mechanism, the damping matrix used in all tests was zero. In this research, the equation of motion was solved step by step by Newmark explicit method.

Two types of devices have been installed between the coupling bar of the amplification system and the reaction slab, corresponding to a frictional damper (AFD [45]) and one mixed (ASD [46]) that adds stiffness and damping. The **Fig.5** and **Fig.6** shows scheme of both devices.

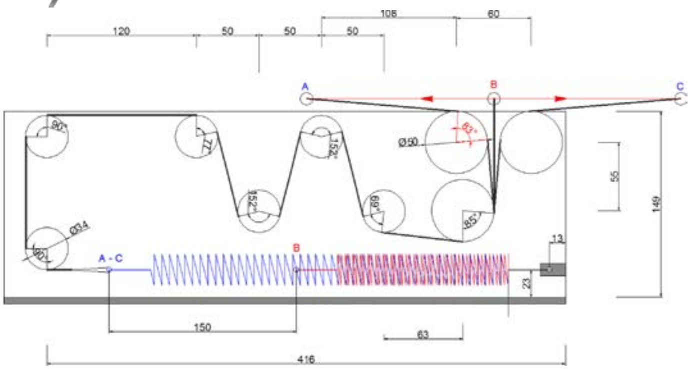

Fig 5: Distribution of elements in ASD-Device I

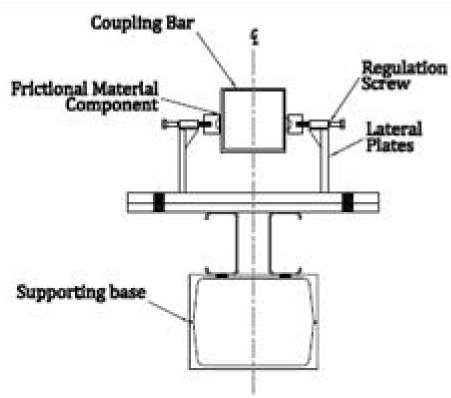

Fig 6: Frictional Damper Scheme (AFD). Device II

4. Experimental Results

Device I

The measured displacements at the axis-A (flexible edge) and axis-E (stiff edge) of the structure without AASD subjected to artificial record with intensity factors (IF) scaled to 10%, 20% and 30%, are presented in **Fig.7a**. As expected, a noticeable concentration of deformation on the flexible edge of the structure was observed. **Fig.7b** shows the results obtained from the structure with the AASD. In this case it was possible to apply up to 70% of the artificial earthquake. Note that the edges deformations are very similar, not only in their maximum values, but also for each time. This is because the stiffening effect of AASD shifts the position of the center of stiffness toward the position of the center of mass (i.e., torsional balance in the strong sense [36, 37]).

Fig.7c shows a comparison between the responses obtained from the structure with and without AASD, subjected to the artificial ground motion with IF = 30%. In this part of the figure the, X-direction global constitutive relations (qx vs Rx) are represented. It can be seen that the AASD causes a reduction of 40% in the displacement qx, but an increase of 10% in the base shear Rx, although a significant part of the base shear is resisted by the AASD, which produce 84% of increment in the X-direction effective stiffness. In the lower chart of part (c) of the figure the combinations of displacement vs plan rotation (qx vs qh) have been represented, where it can be seen not only a significant reduction in the maximum values of the two variables, but also on their statistical correlation, which decreases for 0.81 to -0.02, i.e. practically reached torsional balance condition in a weak sense [36,37].

The strains measures in the four steel rods of the amplifying mechanism of the structure subjected to artificial record with IF = 30%, 50% and 70%, are presented in **Fig. 8**. All rods are prestressed with an initial strain of 200με. Maximum strains occur in the rods 1 and 2, reaching values of 800με, 1300με, 1800με, corresponding to IF = 30%, 50% and 70%, respectively. Note that for IF = 30% the pre-stressing is preserved, while for IF = 50% and 70%, pre-stressing is reduced by approximately 50% and 75% respectively. This is mainly due to partial yielding of steel rod connections.

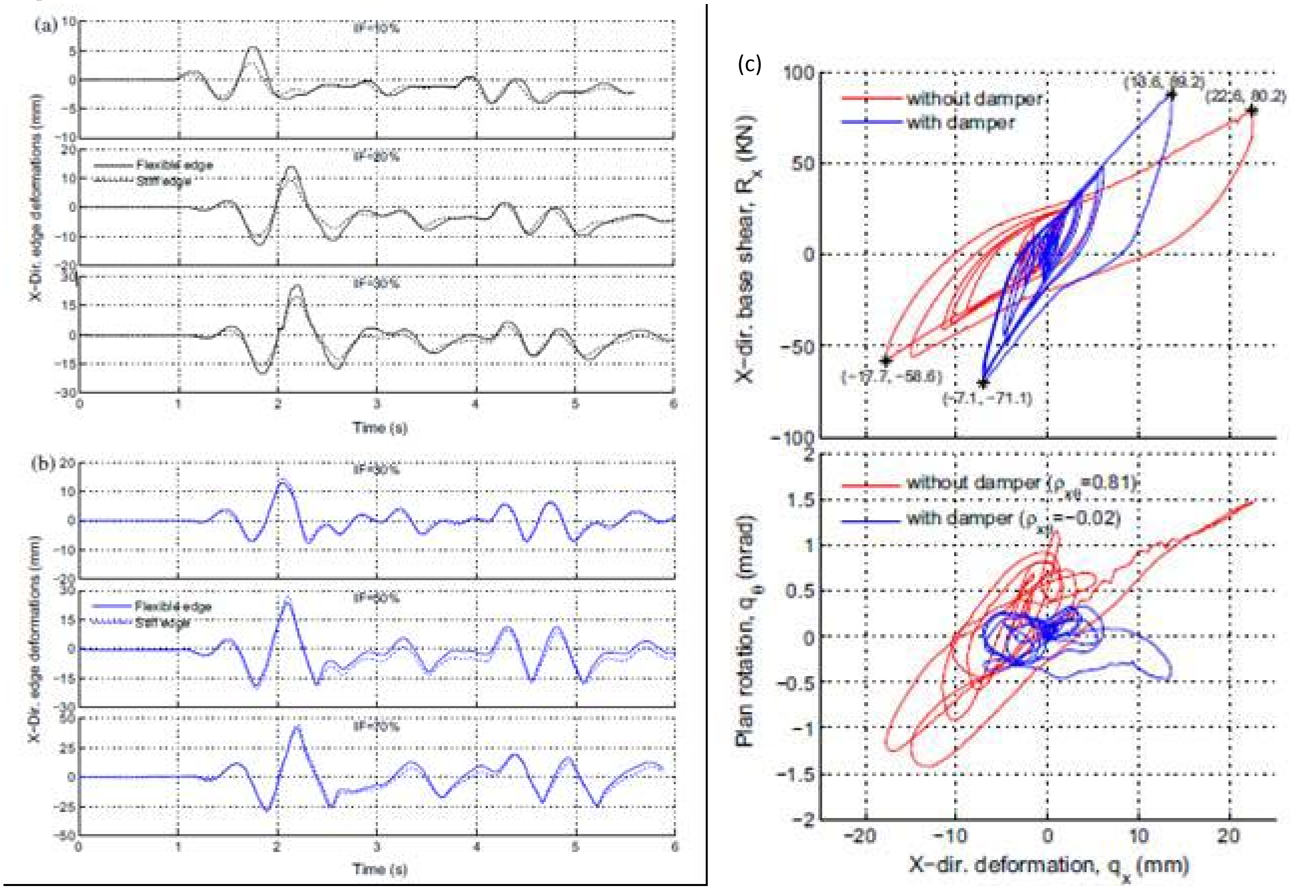

Fig. 7: Measured displacement at the stiff edge (axis-E) and flexible edge (axis-A) of the structure: (a) without AASD (IF = 10%, 20% and 30%); and (b) with AASD (IF = 30%, 50% and 70%); (c) Comparison between the responses of the structure with and without AASD, subjected to the artificial ground motion with IF = 30%.

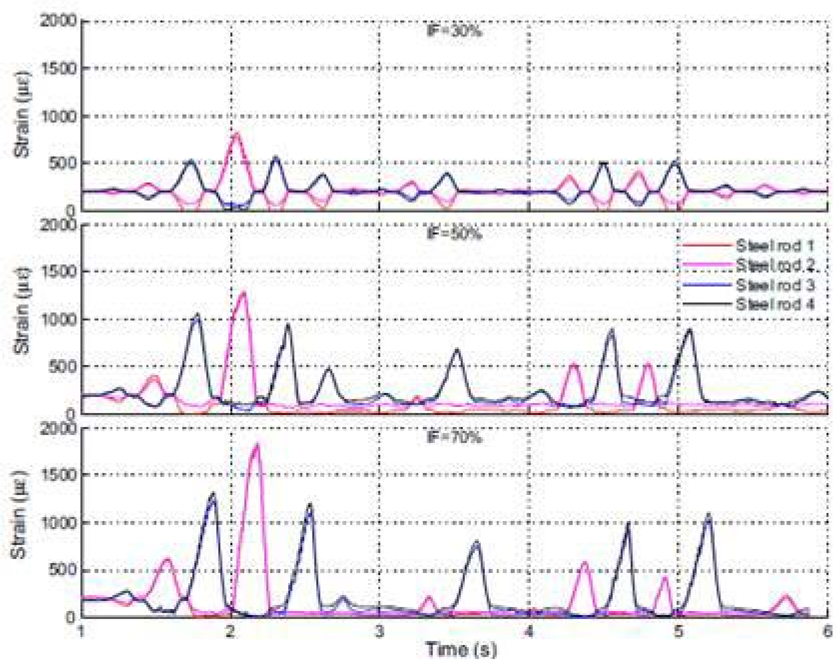

Fig. 8: Measured strains in the four steel rods of the amplification mechanism of the structure with AASD subjected to artificial record with IF = 30%, 50% and 70%.

Device II

As show in **Fig.9a**, the upper graphic shows the difference between the displacements of the two lateral frames. The frame where the amplification mechanism is installed is considered as flexible frame, and the opposite frame is the rigid one.

In order to evaluate the behavior of the structure coupled to the amplification mechanism with the frictional dampers, and compare it with the responses explained in the last paragraph, a second set of tests is developed. The activation force of the frictional damper was set to Q_d = 2,5 KN and the same seismic record specified as the pseudo-dynamic test excitation. This force value was reached after several executions of the test and, is the required force to generate a condition in which both, flexible and rigid frames respond in a similar manner under the seismic excitation. As shown in the lower graphic in **Fig.9b**, for the parameters specified as mentioned before, and for an amplification factor $\alpha \approx 11$ [46], it was possible to reach this balance between the displacement of the two frames, and even decrease the peak response of the steel structure. This response was decreased form a peak of 0,032m to 0,015m, the latter with the amplificator-damper system coupled to the structure. This means a response reduction of approximately 53%. Also, the relation shear force-deformation in the applied seismic record direction is shown in **Fig.9c**. There the response of **Fig. 9a** and **Fig. 9b** can be better understood, relating the decreased displacement to the shear force magnitude which is decreased too, after coupling the structure to the amplificator-damper system.

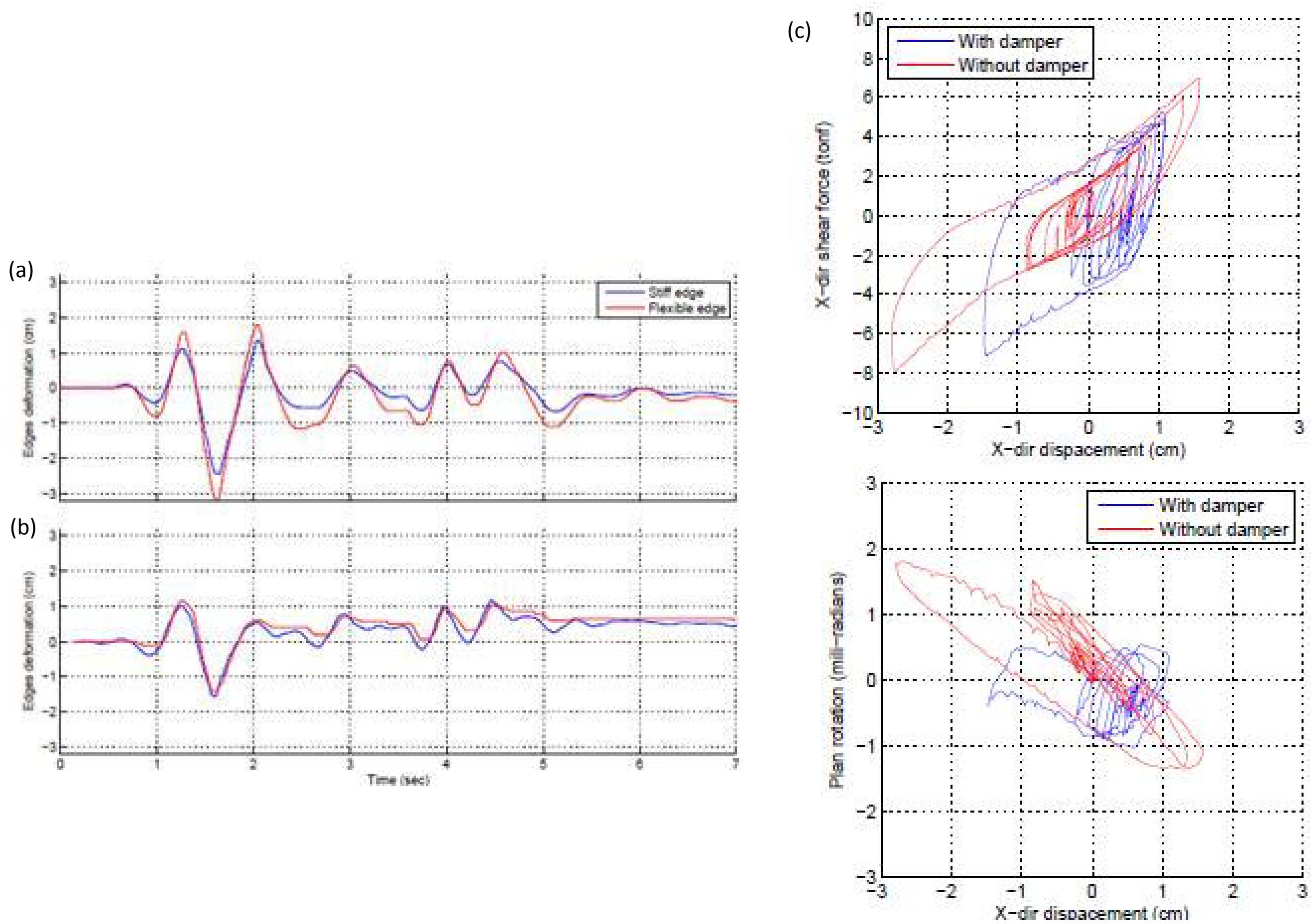

Fig. 9: Comparison of displacement histories for flexible and rigid frames (edges) when; (a) without amplificator-damper system; (b) with amplificator-damper system. Record scaled to 30%, and eccentricity ey = 1:0 m; (c) Comparison between the responses of the structure with and without AAFD, subjected to the artificial ground motion with IF = 30%.

Finally, at the upper graphic in **Fig.10**, the deformation of the damper (plane blue line) and the flexible edge deformation multiplied by the amplification factor of the mechanism (α=11) is shown. Note in this figure that, the reached deformations for the damper are nearly similar to those induced in the structures edge. The horizontal lengths at the peaks of the history plot for the damper deformation, can be explained due to the frictional damper behavior itself, where before reaching a peak deformation value, the device gets stuck and it is necessary to break the friction force again to begin slipping in the counter direction.

Shown in the lower graphic of Figure 20, is the strain history for the tensor bars (T1, T2, T3 and T4) of the amplification mechanism (see Figure 15). Note that the maximum reached strain is of approximately $0{,}58\mathrm{x}10^{-3}$. For this bars, built with mild steel of $F_y = 420$MPa, the yielding strain is measured at $2{,}00\mathrm{x}10^{-3}$, which means that the tensor bars worked in a range of $\gamma_\varepsilon = \varepsilon/\varepsilon_y = 0{,}29$.

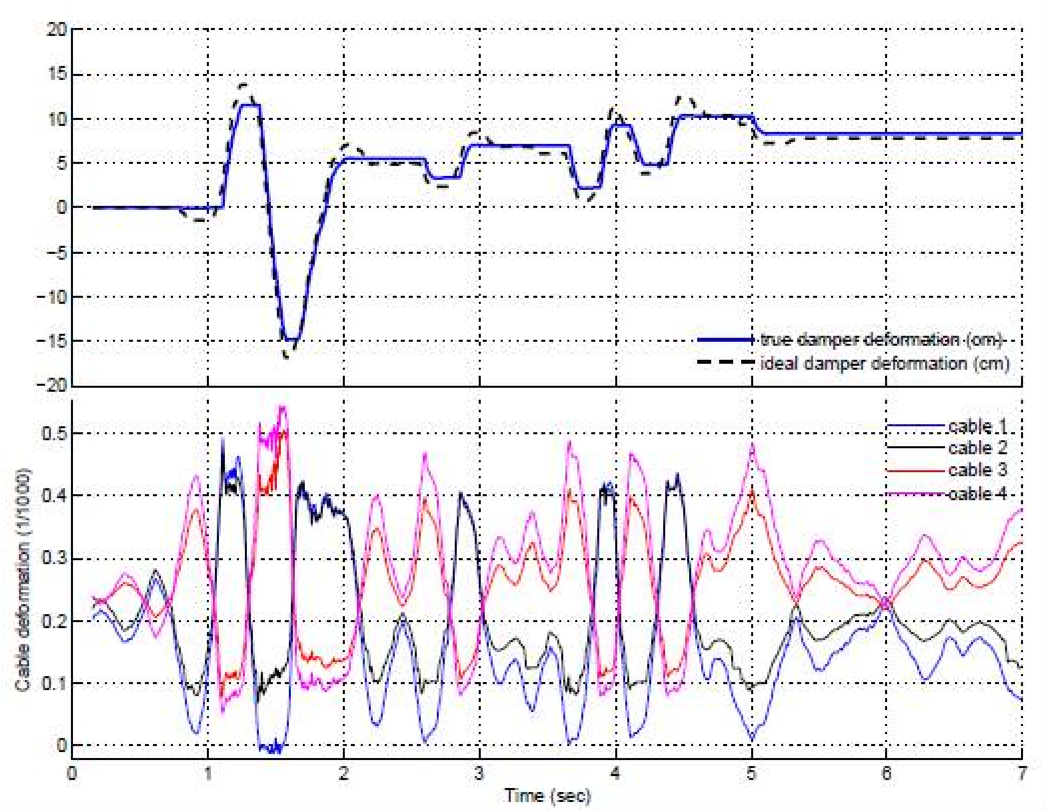

Fig. 10. Response histories with dampers of: (top) real vs "ideal" deformation of the damper; and, (bottom) tensor bars strain measured during pseudo-dynamic test. Record scaled to 30%, and eccentricity $e_y = 1{:}0$ m.

5. Conclusions

A new displacement amplification mechanism, called ELAS, has been proposed. The system admits two possible configurations: (i) a lever-arm and a diagonal bar working in tension and compression; (ii) two lever-arms, two bars or pre-stressed cables working in tension only an a coupling bar. The first of these configurations is very similar to the LAS configuration proposed in [27], which results more appropriate to install only one energy dissipator, ED (concentrated dissipation); while the latter one is useful to connect various EDs (distributed dissipation).

The structure without AM presents a non-linear behavior, mainly due to sliding of the bolted connections of the beams. Pseudo-dynamic seismic response tests were performed considering an artificial ground motion acting in one direction. As expected, and due to the mass eccentricity (25% of the plan length), high concentration of deformations in the flexible edge of the structure without AM was observed.

The eccentric lever arm used as amplifying mechanism, which have large amplifying ratio α=11, worked in great accordance with numerical simulations.
The structure with AAFD showed a great plan deformation uniformity (torsional balance), with reductions of nearly 50% in maximum edge deformation, which is consistent with the results of numerical analysis. The amplification efficiency decreases as the intensity of the earthquake increases. Nevertheless, where the maximum steel rod strain do not exceed $6x10^{-4}$ (approximately 30% of the nominal yield strain) an efficiency of 90% is obtained. In this case a frictional damper with very low force capacity has been used (Qd = 2:5 KN).

The structure with AASD showed a great plan deformation uniformity (torsional balance), with reductions of nearly 40% in maximum edge deformation, which is consistent with the results of parametric analysis. The incorporation of AASD reduces by more than 50% the energy dissipated by the main structure. The amplification efficiency decreases as the intensity of the earthquake increases. Nevertheless, where the maximum steel rod strain do not exceed 800 με (approximately 40% of the nominal yield strain) an efficiency of 77% is obtained.

6. Acknowledgements

This research has been funded by Comisión Nacional de Investigación Científica y Tecnológica (CONICYT) throught the FONDECYT Project No. 1120937 and FONDEQUIP Project EQM120198. The authors are grateful for this support. The authors gratefully acknowledge the support offered by the DictUC crew of the Structural Engineering Department Laboratory in the Pontificia Universidad Catolica de Chile. We also thank Professor Hernán Santa María for providing carbon fibers; laboratory operator Ing. Yoslandy Lazo; Mr. Atilio Muñoz for their support during assembly of the structure; the engineers Jose Luis Ramirez and Ismael Gonzalez of the Company Aries, for their excellent work during the implementation of multi-axis pseudo-dynamic system.

7. References

[1] T. T. Soong and G. F. Dargush, Passive Energy Dissipation Systems in Structural Engineering, New York, USA: John Wiley and Sons Ltd, 1997.

[2] Soong, T.T. and Spencer, B.F. ‘‘Supplemental energy dissipation: state of-the-art and state-of-the practice’’, Engineering Structures, 24(3), pp. 243–259 (2002).

[3] M. D. Symans, F. a. Charney, a. S. Whittaker, M. C. Constantinou, C. a. Kircher, M. W. Johnson, and R. J. McNamara, “Energy Dissipation Systems for Seismic Applications: Current Practice and Recent Developments,” J. Struct. Eng., vol. 134, no. 1, pp. 3–21, 2008.

[4] Kelly, J.M.; Skinner, R.I.; Heine, A.J.; “Mechanisms of Energy Absorption in Special Devices for Use in Earthquake – Resistant Structures”, Bull. N.Z. Nat. Soc. for Earthquake Eng., 5(3), 1972.

[5] K. Tsai, H. Chen, C. Hong and Y. Su, "Design of Steel Triangular Plate Energy Absorbers for Seismic-Resistant Construction," *Earthquake Spectra*, vol. 9, no. 3, pp. 505-528, 1993.

[6] M. Nakashima, "Strain-Hardening Behavior of Shear Panels Made of Low-Yield Steel. I: Test," *Journal of Structural Engineering*, vol. 121, no. 12, pp. 1742-1749, 1995.

[7] M. Nakashima, T. Akazawa and B. Tsuji, "Strain-Hardening Behavior of Shear Panels Made of Low-Yield Steel. II: Model," *Journal of Structural Engineering*, vol. 121, no. 12, pp. 1750-1757, 1995.

[8] S. Kato and Y.-B. Kim, "A finite element parametric study on the mechanical properties of J-shaped steel hysteresis devices," *Journal of Constructional Steel Research*, vol. 62, no. 8, pp. 802-811, 2006.

[9] G. De Matteis, G. Brando and F. Mazzolani, "Hysteretic behaviour of bracing-type pure aluminium shear panels by experimental tests," *Earthquake Engineering & Structural Dynamics*, vol. 40, no. 10, pp. 1143-1162, 2011.

[10] R. W. K. Chan and F. Albermani, "Experimental study of steel slit damper for passive energy dissipation," *Engineering Structures*, vol. 30, no. 4, pp. 1058-1066, 2008.

[11] K. Ghabraie, R. Chan, X. Huang and Y. M. Xie, "Shape optimization of metallic yielding devices for passive

mitigation of seismic energy," *Engineering Structures*, vol. 32, no. 8, pp. 2258-2267, 2010.

[12] A. Benavent-Climent, L. Morillas and J. M. Vico, "A study on using wide-flange section web under out-of-plane flexure for passive energy dissipation," *Earthquake Engineering & Structural Dynamics*, vol. 40, no. 5, pp. 473-490, 2011.

[13] Filiatrault, A.; Cherry, S.; “Performance Evaluation of Friction Damped Braced Steel Frames under Simulated Earthquake Loads”, Earthquake Spectra, 3 (1), EERI, 1987.

[14] Aiken, I.D.; Kelly, J.M.; Pall, A.S.; “Seismic Response of an Nine–Story Steel Frame with Friction Damped Cross–Bracing”, Report No. UCB/EERC – 88/17, EERC, Univ. of California Berkeley, 1988.

[15] C. E. Grigorian, T. S. Yang and E. P. Popov, "Slotted Bolted Connection Energy Dissipators," *Earthquake Spectra*, vol. 9, no. 3, pp. 491-504, 1993.

[16] D. K. Nims, P. J. Richter and R. E. Bachman, "The Use of the Energy Dissipating Restraint for Seismic Hazard Mitigation," *Earthquake Spectra*, vol. 9, no. 3, pp. 467-489, 1993.

[17] Mualla, I.H. & Belev, B., 2002. Performance of steel frames with a new friction damper device under earthquake excitation. Engineering Structures, 24, pp.365–371.

[18] Kim, J., Choi, H. & K.-W., M., 2011. Use of rotational friction dambers to enhance seismic and progressive collapse resisting capacity of structures. The Structural Design of Tall and Special Buildingshe Structural Design of Tall and Special Buildings, 20, pp.515–537.

[19] Constantinou MC, Symans MD. Experimental and analytical investigation of seismic response of structures with supplemental viscous dampers. Tech. Rep. NCEER-92-0032,National Center for Earthquake Engineering Research, Buffalo, N.Y., 1992.

[20] Constantinou, M.C.; Symons, M.P.; Tsopelas, P.; Taylor, D.P.; Fluid Viscous Dampers in Applications of Seismic Energy Dissipation and Seismic Isolation, ATC – 17 – 1, ATC, 1993.

[21] Lee D. and Taylor P. Viscous damper development and future trends, Jhon Wiley & Sons, Ltd. 2001.

[22] M. C. Constantinou, P. Tsopelas, W. Hammel, and A. N. Sigaher, “Toggle-Braced-Damper Seismic Energy Dissipation Systems,” J. Struct. Eng., no. February, pp. 105–112, 2001.

[23] D. P. Taylor and M. C. Constantinou, "Development and Testing of an Improved Fluid Damper Configuration for Structures Having High Rigidity," New York, USA, 2004.

[24] Hwang, J., Huang, Y. and Hung, Y. ‘‘Analytical and experimental study of toggle-brace-damper systems’’, Journal of Structural Engineering-ASCE, 131(7), pp. 1035–1043 (2005).

[25] Jenn-Shin Hwanga, Chun-Hsiang Tsai, Shiang-Jung Wang, Yin-Nan Huang. Experimental study of RC building structures with supplemental viscous dampers and lightly reinforced walls. Engineering Structures 28 (2006) 1816–1824.

[26] A. N. Şigaher and M. C. Constantinou, “Scissor-jack-damper energy dissipation system,” Earthq. Spectra, vol. 19, no. 1, pp. 133–158, 2003.

[27] Y. Ribakov and A. M. Reinhorn, “Design of Amplified Structural Damping Using Optimal Considerations,” J. Struct. Eng., vol. 129, no. October, pp. 1422–1427, 2003.

[28] T. S. K. Chung and E. S. S. Lam, Hydraulic Displacement Amplification System for Energy Dissipation. 2004.

[29] S. Berton and J. E. Bolander, “Amplification System for Supplemental Damping Devices in Seismic Applications,” J. Struct. Eng., vol. 131, no. June, pp. 979–983, 2005.

[30] McNamara, R.J., Huang, C. and Wan, V. Viscous damper with motion amplification device for high rise building applications, Advanced Technology in Structural Engineering, ASCE Structures Congress, Philadelphia, PA, USA (2000).

[31] DeSimone, S. and Steven, B. Long back spans, upturned spandrels and toggle brace-dampers meet the complex seismic requirements of the irregularly shaped steel tower for San Francisco’s Four Seasons Residences. Modern Steel Construction, American Institute of Steel Construction, Chicago, USA (2002)

[32] Goel RK, "Effects of supplemental viscous damping on earthquake response of asymmetric-plan systems," Earthquake Engineering & Structural Dynamics, vol. 27, no. 2, pp. 125-141, 1998.

[33] Lin WH, and Chopra AK, "Understanding and predicting effects of supplemental viscous damping on seismic response of asymmetric one-storey systems," Earthquake Engineering & Structural Dynamics, vol. 30, no. 10, pp. 1475-1494, 2001.

[34] Goel RK. Seismic response of linear and non-linear asymmetric systems with non-linear fluid viscous dampers.

Earthquake Engineering and Structural Dynamics 2005; 35:825–846.

[35] J. C. De la Llera, J. L. Almazán and I. J. Vial, "Torsional balance of plan-asymmetric structures with frictional dampers: analytical results," Earthquake Engineering & Structural Dynamics, vol. 34, no. 9, pp. 1089-1108, 2005.

[36] Almazán J.L., and De la Llera J.C. Torsional balance as new design criterion for asymmetric structures with energy dissipation devices. Earthquake Engineering and Structural Dynamics. (38) 1421-1440, 2009.

[37] Aguirre J ., Almazán J., and Paul C. Optimal control of linear and nonlinear asymmetric structures by means of passive energy dampers. Earthquake Engineering and Structural Dynamics, 42 (3) 377-395, 2013.

[38] I. J. Vial, J. C. De la Llera, J. L. Almazán and V. Ceballos, "Torsional balance of plan-asymmetric structures with frictional dampers: experimental results," Earthquake Engineering & Structural Dynamics, vol. 35, no. 15, pp. 1875-1898, 2006.

[39] M. García, J. C. De la Llera and J. L. Almazán, "Torsional balance of asymmetric structures with viscoelastic dampers," Engineering Structures, vol. 29, no. 6, pp. 914-932, 2007.

[40] A. Mokha, M. Constantinou and A. Reinhorn, "Teflon Bearings in Base Isolation. I: Testing," *Journal of Structural Engineering* , vol. 116, no. 2, pp. 438-454, 1990.

[41] A. Mokha, M. Constantinou and A. Reinhorn, "Teflon Bearings in Base Isolation II: Modeling," *Journal of Structural Engineering,* vol. 116, no. 2, pp. 455-474, 1990.

[42] J. B. Roberts and P. D. Spanos, Random Vibration and Statistical Linearization, Chichester, England: John Wiley & Sons, Ltd., 1990.

[43] J. Hancock, J. Watson-Lamprey, N. A. Abrahamson and J. J. Bommer, "An improved method of matching response spectra of recorded earthquake ground motion using wavelets," Journal of Earthquake Engineering , vol. 10, no. 1, pp. 67-89, 2006.

[44] Yuri Ribakov and Andrei M. Reinhorn. Design of Amplified Structural Damping Using Optimal Considerations. Journal of Structural Engineering, 129(October):1422–1427, 2003.

[45] Baquero J., Almazán J., and Tapia N. Amplification system for concentrated and distributed energy dissipation devices. Earthquake Engineering and Structural Dynamics. (45) 935–956, 2016.

[46] Tapia N., Almazán J., and Baquero J. Development of a novel combined system of deformation amplification and added stiffness and damping: Analytical result and full scale pseudodynamic tests. Engineering Structures 119 (2016) 61-80.

[47] L. Al-Atik and N. Abrahamson, "An Improved Method for Nonstationary Spectral Matching," Earthquake Spectra, vol. 26, no. 3, pp. 601-617, 2010.

[48] Norma NCh.2745, Análisis y diseño sísmico de edificios con aislación sísmica, Chile: INN, 2003.

[49] H. M. Aktan, "Pseudo-Dynamic Testing of Structures," *Journal of Engineering Mechanics,* vol. 112, no. 2, pp. 183-197, 1986.

[50] S. A. Mahin and P.-S. B. Shing, "Pseudo dynamic method for seismic testing," *Journal of Structural Engineering,* vol. 111, no. 7, pp. 1482-1503, 1985.

[51] M. Nakashima and H. Kato, "Experimental Error Growth Behavior and Error Growth Control in On-Line Computer Test Control Method.," Building REsearch Institute, Ministry of Construction, Japan, 1987.

[52] M. Nakashima, "Integration techniques for substructure pseudo dynamic test," in *4th U.S. National Conference on Earthquake Engineering II*, Palm Springs, CA, USA, 1990.

[53] M. Nakashima, T. Akazawa and H. Igarashi, "Pseudo-dynamic testing using conventional testing devices," *Earthquake Engineering & Structural Dynamics,* vol. 24, no. 10, pp. 1409-1422, 1995.

[54] J. Donae, G. Magonette, P. Negro, P. Pegon, A. Pinto and G. Verzeletti, "Pseudodynamic Capabilities of the ELSA Laboratory for Earthquake Testing of Large Structures," *Earthquake Spectra,* vol. 12, no. 1, pp. 163-180, 1996.

[55] P. Negro, "Verification of the Pseudodynamic Test Method.," *European Earthquake Engineering* , vol. 12, no. 1, pp. 40-50, 1998.